Toxicology Reports 9 (2022) 470–479

Contents lists available at ScienceDirect

Toxicology Reports

journal homepage: www.elsevier.com/locate/toxrep

Radioiodination of zearalenone and determination of *Lactobacillus plantarum* effect of on zearalenone organ distribution: In silico study and preclinical evaluation

M.H. Sanad [a], A.B. Farag [b], Sabry A. Bassem [c,*], F.A. Marzook [a]

[a] Labeled Compounds Department, Hot Labs Center, Atomic Energy Authority, P.O. Box 13759, Cairo, Egypt
[b] Pharmaceutical Chemistry Department, Faculty of Pharmacy, Ahram Canadian University, Giza, 12578, Egypt
[c] Food Toxicology and Contaminants Department, National Research Centre, Dokki, Cairo, PB12622, Egypt

ARTICLE INFO

Handling Editor: Dr. Aristidis Tsatsakis

Keywords:
Radioiodination
Zearalenone
Protective effect
Lactobacillus plantarum
Organ toxicity

ABSTRACT

Purpose: Zearalenone (ZEN) which is one of the known fusarium species mycotoxin, produced primarily on many cereal crops. Consequently, the current study aims to estimate the possibility of labeling zearalenone and the pattern of accumulation of the produced labeled zearalenone [^{125}I]-ZEN in different mice tissues, and the possible protective effect of *Lactobacillus plantarum* to reduce organ accumulation of Zearalenone.
Materials and methods: the experiment was conducted on two groups of mice were used; the two groups received [^{125}I] Zearalenone administered by tail vein injection, the first group receive nothing else while the second group received also *L. plantarum* (as a control agent) orally. The mice were kept under observation for 120 min to monitor zearalenone distribution.
Results: by monitoring the zearalenone distribution the maximum concentration was found to be mainly primarily in the intestine (45.8 %) followed by the liver (27.15 %) while in the ovary (the most susceptible organ was (3.22 %) after120 min, in the first group of mice. The same pattern was observed in the second group with concentrations of (46.1 %), (30.19 %) and (0.09 %) in the intestine, liver respectively.
Conclusion: These results indicated the lactic acid bacteria played a role in decreasing labeled zearalenone in the ovaries which is the target organ. [^{125}I]-labeled ZEN is a promising novel tracer for organ imaging and that a significant role that *L. plantarum* could play in decreasing the zearalenone bioavailability of in mice organs.

1. Introduction

Zearalenone (ZEN) is considered one of the major mycotoxins produced by fusarium species, and is formed primarily on many cereal crops which are considered the main host plants primarily in the field, but several reports indicated its presence during poor grain storage conditions. Zearalenone (ZEN) belongs to resorcyclic acid lactone mycotoxins (Fig. 1)

The climatic conditions is considered one of the controlling factors of the natural occurrence of zearalenone [1]. reported the increase of the natural occurrence of ZEN as a result of climatic changes in relation to rain fall as, the increase of Rainfall accompanied by moderate temperatures throughout the blossoming and maturation seasons were found to increase cereals infestation (mostly *Triticum* and *Zea mays*) with *Fusarium culmorum* and accordingly Zearalenone infestation. The variation of concentrations of zearalenone in maize from one year to the other is mostly associated with rainfall. ZEN concentrations were remarkably elevated in maize collected in the period from 2014 to 2017 in Central Europe. Also in Southern European, while levels ZEN were relatively elevated in maize harvested in the same period opposite observations In East Asian maize, as the levels of ZEN were comparatively low in maize harvested at the same time these results shed light on the increasing importance of ZEN with the occurring climate changes nowadays.

ZEN is usually called (an estrogenic mycotoxin) which causes obvious estrogenic effects in both human and animals, which is a direct result to the structural similarity to the natural estrogens. The IARC has considered ZEN to be Group 3 carcinogen. As a result of its strong hazardous effects a lot of public health concerns arise. ZEN binds competitively to estrogenic receptors (ERα and ERβ) in many in vitro or in vivo systems in different species, causing serious malignant

* Corresponding author.
E-mail address: Bassemsabry2004@gmail.com (S.A. Bassem).

https://doi.org/10.1016/j.toxrep.2022.02.003
Received 31 May 2021; Received in revised form 21 January 2022; Accepted 6 February 2022
Available online 11 February 2022

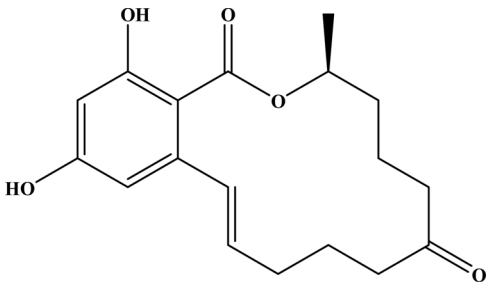

Fig. 1. Chemical structure of zearalenone.

alterations and lesions in the female reproductive system [2].

Iodine-131 is one of the most used isotopes used therapeutically for hyperthyroidism and it is also considered as one of the first radiotracers used in nuclear medicine. The principal releases of iodine-131 decay are electrons, with a maximum energy of 606 keV (89 % abundance, others 248–807 keV) and 364 keV gamma radiation (81 % abundance). That's why, it's not recommended to be utilized in optimum conditions or bio distribution just in case of the presence of its high energy with beta emission. Therefore, we preferred to use Iodine-125 for the development of all our study due to the fact that it is characterized by its low energy (about 35 Kev). Iodine-125 is the isotope of choice for medical imaging with a half-life to 59.49 days and decays by electron capture to an excited state of tellurium-125 (not the metastable state). That decays immediately by gamma decay to give Iodine-125 with a maximum energy of 35 keV The toxicity of deoxynivalenol was evaluated via the administration of [^{125}I] - labeled deoxynivalenol in mice [3].

One of the most promising technique in prevention of mycotoxin hazardous effects is via the use of lactic acid bacteria, Lactic acid bacteria (LAB) are a large species of gram-positive bacteria the majority of which are non- movable rods and cocci. LAB usually get its carbohydrates needs through fermentation forming lactic acid which is considered its end product [4]. LAB are extensively engaged in the fermentation processes of food and feed, which add extensively to its hygienic and safety characteristics, storage constancy and desirable physical properties [5] and [6]. One of the main benefits of these bacteria it the fact that LAB are of great importance in their usage in the bio-preservation of human food and animal feed, and that is essentially attributed to its ability to produce natural antimicrobial compounds. *Lactobacillus plantarum* usually found abundantly all over the environment with wide-ranging of uses *L. plantarum* safe utilization has a long history in a variety of food products especially with human gastrointestinal tract (GIT) being its normal host. Several studies investigated *L. plantarum* strains and results supported the fact that LAB possess substantial capability to inhibit many undesirable bacteria, including both Gram negative and Gram positive species, that may infect food causing diseases in humans. These strains preserve a significant ability to counteract numerous undesirable bacteria, including both Gram-negative and Gram-positive species that can infect food causing sicknesses in humans. The biosynthesis of many metabolites (organic acids, enzyme systems, and bioactive peptides ….etc) is a suggested mechanism for the antimicrobial, antioxidant, properties of probiotic bacteria which enables it to act as natural preservatives agents against pathogenic microorganisms that may affect food quality during food process from harvest to human. Which in turn decrease the need for chemical preservatives, increasing health and safety and decreasing the risks for the consumer.

A lot of researches revealed that various species of LAB have the ability to eliminate mycotoxins. The ability of LAB for the removal vary from small amounts up to complete elimination [7–12]. The species that showed the best activities were *Lactobacillus rhamnosus, L. acidophilus, L. plantarum, L. lactis, Streptococcus thermophilus,* and *Bifidobacterium bifidum.* While the activity of the different spices differ according to the type of the mycotoxin yet *L. rhamnosus,* was found to have the ability to eliminate several mycotoxins at the same time [9,13–16].

That is why, the aim of the current work was to clarify the distribution of [^{125}I]-labeled ZEN in mice organs, and the possible role of *Lactobacillus plantarum* as a protector against Zearalenone organ toxicity.

2. Materials and methods

2.1. Chemicals and reagents

Zearalenone (ZEN), chloramines-T (Ch-T), ethanol and methanol were acquired from Sigma-Aldrich. Aluminum sheets thin layer chromatography (TLC) plates (20 × 25 cm) SG-60 F254 from Merck. All the chemical substances used in this study were of analytical or clinical grade & were directly used no more purification except else was stated. No-carrier-added (NCA) [^{125}I] as NaI (185 MBq/50 μL) diluted in 0.04 M NaOH, pH 9–11 was supplied by the institute of isotopes, Hungary, >99 %. For radioactive measurement A well-type NaI scintillation γ-Counter model Scalar Ratemeter SR7 (Nuclear Enterprises Ltd., USA) was used. The mixture was completely purified using High Performance Liquid Chromatography HPLC column, provided with a Shimadzu model detector SpD-6A (SHIMADZU Cooperation, MD, USA) that contains LC-9A pumps, column Lichrosorb (RP-C18−250 mm × 4.6 mm, 5 μm)., rheodyne injector and UV spectrophotometer detector at 320 nm wavelength. At the optimal conditions an injection of 10 μ from the [^{125}I] ZEN solution was injected in the HPLC. As recommended methanol: water (9:1,v/v/), was The mobile phase moving at 1.0 mL/min rate. Fractions were collected separately from a 1.0 mL volume up to 15 mL volume and counted with a γ-ray scintillation counter [17,18].

2.2. Radiolabeling process

We used a fixed volume of the reaction mixture (approximately ~ 720 μL). Divided on a 2- round bottom flasks (25 ml) each fitted with a reflux condenser and a rubber septum immersed in a thermostatically controlled water bath was added [^{125}I] NaI (7.2 MBq in 0.1 % NaOH) and vaporized to dryness. 100 μg Ch-T was accurately weighed then dissolved in ethanol (1 mg: 1 mL) then added to the reaction flask, after that (50 μg) ZEN was dissolved in ethanol at a ratio of (1 mg: 1 mL). All the mixture was mixed thoroughly with a magnetic stirrer at 37 °C for 20 min. After that to get rid of the extra of iodine 150 μg of (60 mg/mL H2O) sodium metabisulphite was added to stop the reaction. The radiochemical conversion to [^{125}I] iodo ZEN was established using TLC method. 2 μL (1.70 MBq) of the reaction mix spotted just above the lower rim of aluminum-backed silica gel GF254 plates, after that it was left to vaporize. methylene chloride ethyl acetate (2:1 was used as the mobile phase for the development of the plate, then the plate was left to dry then divided into 1 cm sections and were examined for radioactivity using SR.7 gamma counter. HPLC analysis revealed a purity for [^{125}I] iodo ZEN up to <99 % after ensuring complete purification Fig. 2(a, b &c) [19–55].

2.3. Determination of [^{125}I] ZEN stability

The stability of [^{125}I] ZEN was determined using two different media, saline and serum: In rat serum, 0.1 mL of the radiotracer was mixed with 1.9 mL of serum [0.18 MBq] and stored at 37 °C. The next experiment, the radiotracer of [^{125}I] ZEN [5 μL (3.60 MBq)] was checked in saline., the stability of [^{125}I] ZEN in both media was established by TLC technique at different times, and counted in a well-type γ-scintillation counter [19–23].

2.4. Preparation of the used Lactobacillus plantarum

Lactobacillus plantarum was obtained from the department of Dairy

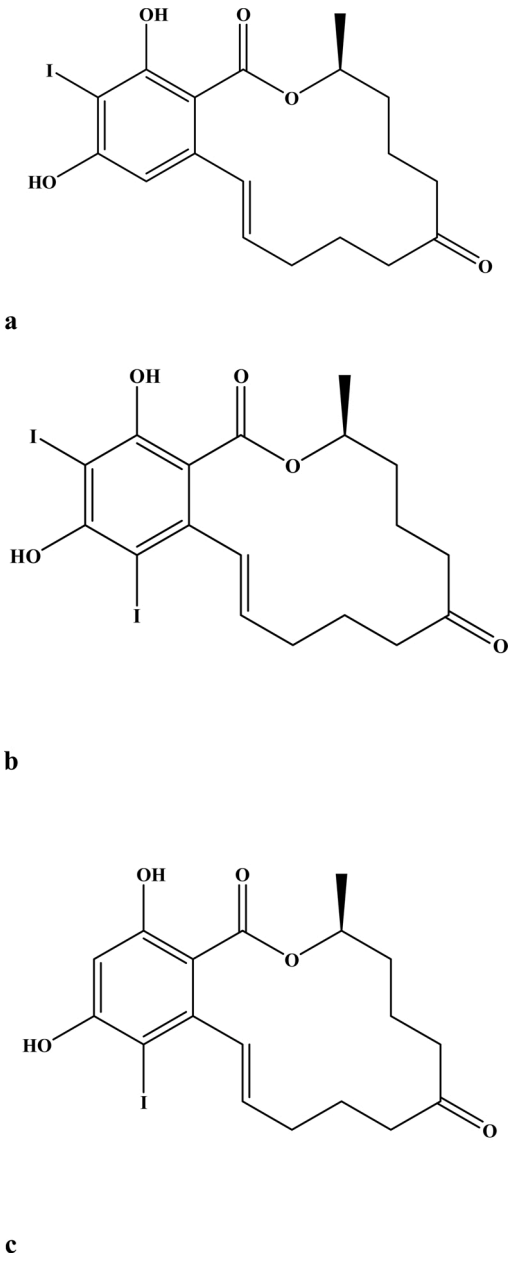

Fig. 2. (a) Possible Chemical structure of Iodozearalenone (b) Possible Chemical structure of Iodozearalenone. (c) Possible Chemical structure of Iodozearalenone.

Science, National Research Centre. According to the method described by [18] as follow the strain was stored in De Man Rogosa Sharpe broth (MRS, Conda, Spain).*Lactobacillus plantarum* was sub-cultured twice in MRS broth before experimental use. Cells were removed by centrifugation at 10,000gfor 5 min, washed three times; freeze-dried. Each tube of prepared *L. plantarum* was frozen at–80 C for 8 h and then freeze-dried for 24 h. After the end of the freeze-drying cycle, the tubes were sealed under vacuum and stored at 20 °C. Frozen samples were re-suspended in sterile phosphate buffer saline(PBS, PH 7.0), and serial dilutions (101 to 109) were pre-pared in 0.1 % tryptone, placed on MRS agar medium and incubated at 37 °C for 24 h. The number of viable cells was determined as colony forming unit per milliliter (CFU/mL).

2.5. Bio distribution of [^{125}I] ZEN in mice

The total experiment was conducted on a total of 50 mice (Swiss Albino mice) weighted (30−35 g) the mice were acclimatized for 1 week, then were divided into two groups (25mice/group). Group 1, treated intravenously with [^{125}I] ZEN 0.2 mL ([^{125}I] NaI, 7.5 MBq, and group 2, treated intravenously with [^{125}I] ZEN and orally with *L. plantarum* suspension (30 mL/kg b.w.) for two weeks. scarification of animals was conducted after certain times (5 min, 15 min, 30 min, 60 min and 2 h) after injection. Organs were collected in addition to (Fresh blood, bone, and muscle tissues) then measured against prepared standard solution of the labeled substrate [56–100]. The mean percentage of the injected dose was calculated. The blood, bone, and muscles were anticipated to represent about 7, 10, and 40 % of the total body weight, respectively. Adjustments were done for background radiation and decay during the experiments. The data were analyzed statistically with one way Analysis of variance ANOVA test with $P < 0.05$.

2.5.1. Ethical considerations

All the animal experiments were carried out in compliance with the standards set out by the Animal Ethics Committee, Labeled Compounds Department-Egyptian Atomic Energy Authority (EAEA).

2.6. In silco study

The x-ray crystallographic structure of estrogen receptor alpha (ERα) (PDB code: 5krc) bound to earalenone which was taken from Protein Data Bank RCSB website [www. rcsb. Org] (Research Collaboration for Structural Bioinformatics) was used to perform the docking studies. Chains B, C and D were deleted and chain A was prepared using the Structure Preparation application in Molecular Operating Environment (MOE), Then the protonate 3D application was used to add the missing hydrogens and assign the ionization states [24–26].

3. Results

3.1. TLC and HPLC estimate of radiochemical yield

The total yield of the radiotracer consists of free [^{125}I] -iodide and [^{125}I] -ZEN it is calculated from the percentage (%), on TLC at RTs (retention times) 0.0 and 0.9–1.0 respectively. HPLC analysis revealed the following, the purity for [^{125}I]-ZEN reached 99 % [101–120]. The Retention times values for both the free iodide and the labeled molecule [^{125}I]-ZEN existed at 4.5 and 15.8 min, respectively, with regard to the retention time for ZEN that was 14.7 min (Fig. 3).

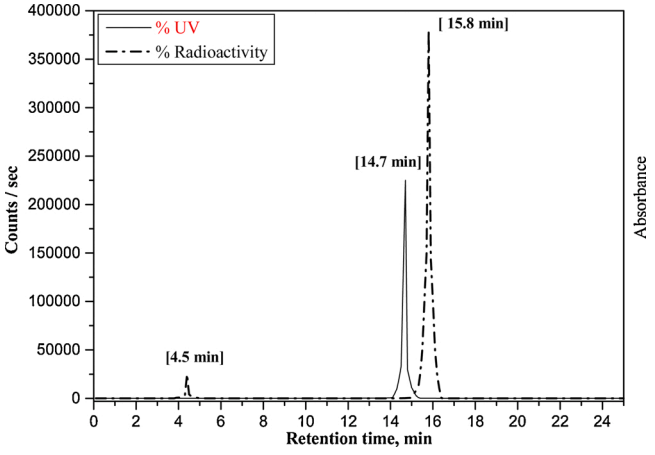

Fig. 3. HPLC radiochromatogram of ^{125}I-zearalenone and its UV at optimum conditions.

3.2. Optimization

Effect of ZEN concentration: The quantity of substrate may influence the radiochemical yield as a function of ZEN concentration that was cleared in (Fig. 4a). In which the radiochemical yield was increased to 98.0 ± 0.29 % by increasing the amount of ZEN up to 50 μg. The substrate beyond 50 μg not affecting on the radiochemical yield [24,25]. It is important remembered that Chloramine-T have the ability to serve as an oxidizing agent, in both acidic and alkaline media, that also related with the nature of active oxidizing species according to the medium pH and the reaction conditions. Therefore, when chloramine-T was dissolved in water, then decomposed to ArSO2NCl, that is hydrolyzed in acidic medium giving HOCl. In addition, further hydrolysis of the hypohalous acid gave H2OCl+. But in alkaline solutions, Ch-T gave the following species HOCl and ClO. The HOCl or H2OCl + generated can (under acidic conditions) cause iodine oxidization leading to the formation of the oxidative state I+ (iodonium) and consequently reacts with any active sites within thiazole ring (in this case only on site present) that can undergo electrophilic substitution reaction. Effect of chloramine-T (Ch-T) concentration: is considered one of the most oxidizing agent used due to its capacity to oxidize the iodide (I-) leading to generate the extremely reactive, electrophilic species (H2OI + and HOI) that have vital part in the iodination reaction. Therefore, the quantity of chloramine-T used is of great importance in the iodination process. The yield of radioiodinated ZEN increases by increment of chloramine-T quantity from 25 to 100 μg (optimum concentration) leading to the formation of highest radiochemical outcome of 98.0 ± 0.29 as shown in (Fig. 4b). Effect of reaction time: From the obtained results demonstrated in (Fig. 4c). It was concluded that the radiochemical yield of radioiodinated ZEN at different times ranging from 5 to 60 min giving maximum radiochemical yield at 30 min of 98.0 ± 0.29. Effect of pH: The changing in pH was demonstrated graphically as illustrated in (Fig. 4d). At pH 6, the yield was maximized (98.0 ± 0.29 %) as a result of the immense stability of radioiodinated ZEN structure at this pH value giving H+, which was easily replaced by the active iodonium ion I + . two different medium were used to study In-vitro stability of radioiodinated ZEN. results revealed that radioiodinated ZEN have high stability in saline up to 48 h. On the other hand different results were obtained in serum, as the stability was only up to 24 h giving 93.2 % (Fig. 5).

3.3. Biodistribution of [^{125}I]-ZEN

Records presented in Table 1 showed the bio-distribution of [^{125}I]-iodo ZEN in various organs and fluids of the body. All radioactivity levels were stated as an average percentage of injected dosage/gram tissues (%ID/gram). [^{125}I]-iodo ZEN rapidly accumulated in the blood (13.00 %), liver (14.6 %), intestine (12.40 %), kidneys (5.17 %), and ovary (2.50 %) 5 min following the injection, while minor quantities were recorded in the brain (0.78 %). There was marked increment of the concentration in liver after 60 min reaching about 38.24 % followed by obvious decrement in the concentration recording 27.15 % after 120 min. This observations shown that the excretion of the tracer was via the hepatobiliary pathways. After 60 min, the [^{125}I]-iodo ZEN amount declined in the blood to (1.10 %), bone (0.90 %), heart (0.80 %), and lungs (0.81 %), kidneys (3.11 %), and liver (27.15 %).while after 30 min The accumulation of the [^{125}I]-iodo ZEN amount in ovary recorded 8.8 % with an observed decrement to 3.22 % after 2 h

3.4. Influence of L. plantarum on the biodistribution of [^{125}I]-ZEN

Records in (Table 2) indicated that the accumulation of [^{125}I]-ZEN in the mice tacking *L. plantarum* did not reduced significantly. [^{125}I]-ZEN distribution was: in blood (13.90 %), liver (12.15 %), intestine (11.50 %), followed by lungs (1.14 %), and ovaries (0.11 %) 5 min following injection. These records were lower than those reported in the group of control mice receiving only [^{125}I]-ZEN, which support the claims about the *L. plantarum* ability to reduce the accumulation of [^{125}I]-ZEN. It was also observed that [^{125}I]-ZEN accumulation declined in the ovaries with time (15, 30, 60, and 120) min in mice treated previously with *L. plantarum*.

4. Discussion

Nowadays human health suffer from exposure to several types of pollutants that vary in its nature as well as its effects, some of these pollutants are due to industrialization, and unfortunately others are naturally produced and mostly unavoidable such as mycotoxins. Zearalenone is a mycotoxin that could be categorized as environmental pollutant that infest grain crops worldwide. It is extensively repo1rted in food and feed having hazardous effects on health of animals and human beings [29–31]. Investigation confirmed that ZEN and ZEN metabolites generally react on oestrogen target organs causing reproductive syndromes in animals and grave oestrogen disorder in humans [29]. Nevertheless, most of the previous records focused on its estrogenic effects only giving lesser concern to the fact that other organs could be also affected by Zearalenone through its bio-distribution. The present study, showed clearly the bio-distribution of labeled ZEN in different organs and fluids of mice following the pattern; Blood- > liver > intestine > muscle > kidney > ovary > lung. Labeled ZEN initially declined at a fast rate during the 1 st 120 min in all tissues except for kidney, intestine, and liver. The highest radiochemical yield was determined using different ZEN concentrations which revealed that the maximum radiochemical transformation to [^{125}I]-iodo ZEN was 98.0 % at 50 Micrro gram ^{l}g of the substrate. These findings differ from those reported by previous studies [32,39] who reported that the after 24 h purity declined to 89.0 %. The study of the biodistribution of [^{125}I]-iodo ZEN revealed that [^{125}I]-iodo ZEN rapidly accumulate in the blood, liver, intestine, and kidney. Such results follow the same pattern as the results of previous reports [39] and [40] who reported that the accumulation of ^{125}I-labeled deoxynivalenol in the liver and kidney was observed following intravenous administration in mice. Another report by [41] revealed the presence ZEN in the rats, ZEN was found in kidneys, liver, and lung after intravenous administration. According to the International Agency for Research on Cancer (IARC), zearalenone belongs to group No. 3, which includes mycotoxins that are not classified as carcinogenic to humans [42]. The toxicity of ZEN in vivo was studied by many research mostly reported the hazardous effect of Zearalenone on the reproductive systems either in male or female [42], also there was a specific concern about the lipid peroxidation of membranes which is included in the means by which ZEN exert its toxic action on human [413, another concern was the findings of [44] who demonstrated the ability of Zearalenone to disrupt liver functions and affect the liver thoroughly to the degree of suppression of cytochrome P450 in the liver results of our work gave clear data about the distribution of Zearalenone in different body organs which in turn could reveal the most susceptible organs that could suffer from Zearalenone/derivatives toxicity [121–145]. By examining the beneficial effect of *L. plantarum* on the organ exposure to Zearalenone/derivatives, results revealed that although the administration of *L. plantarum* did not significantly alter the accumulation of [^{125}I]-iodo-ZEN in different mice organs and there were observed similarity in the pattern of Zearalenone distribution through different organs yet there was marked reduction in the Zearalenone concentration in the ovary and that was observed from the 1st 5 min of administration, and since the ovaries are considered the most sensitive (target) organ of Zearalenone toxicity that could provide additional benefit for the use of LAB as it was reported to demonstrate anti-inflammatory, anti-genotoxic and improve ovarian fertility [45], the decline in the accumulation of [^{125}I]iodo ZEN in mice organs may be attributed to the lactic acid bacterial capability to bind and/or alter ZEN to other compound [9]. Which in turn could result in the decrement of the ZEN in the ovaries leading to the reduction in their related estrogenic

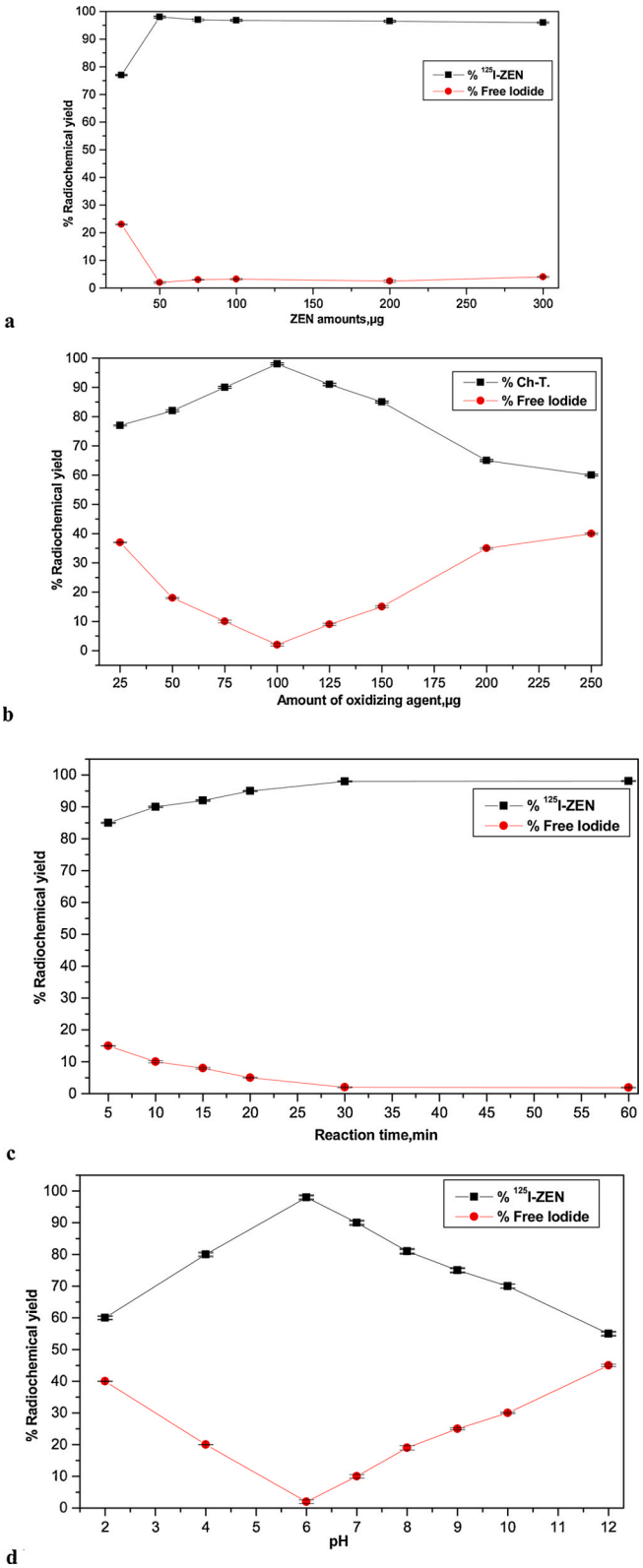

Fig. 4. (a) Variation of the radiochemical yield of radioiodinated ZEN as a function of different ZEN amounts; reaction conditions: 10 µl (~3.7 MBq) $Na^{125}I$, (x µg) olmesartan, 100 µg of Ch-T, at pH 6, the reaction mixtures were kept at room temperature for 30 min. (b) Graph showing the effect of different oxidizing agent amount on the radiochemical yields under the reaction conditions: 10 µl (~3.7 M Bq) $Na^{125}I$, 100 µg of ZEN, (x µg) of Ch-T, at pH 6, the reaction mixtures were kept at room temperature for 30 min. (c) Variation of the radiochemical yield of radioiodinated ZEN as a function of reaction time; reaction conditions: 10 µl (~3.7 MBq) $Na^{125}I$, 50 µg of ZEN,100 µg of Ch-T, at pH 6, the reaction mixtures were kept at room temperature for different intervals of time. (d) Variation of the radiochemical yield of radioiodinated ZEN as a function of pH; reaction conditions: 10 µl (~3.7 MBq) $Na^{125}I$, 50 µg of ZEN, 100 µg of Ch-T, at different pH, the reaction mixtures were kept at room temperature for 30 min.

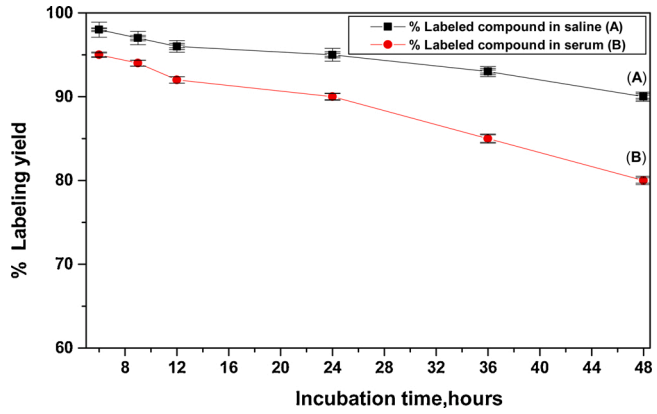

Fig. 5. In vitro stability of 125I- ZEA at optimum condition in saline (A) and serum (B).

influence [46]. Established the ability of some lactic acid bacterial strains to remove ZEN and its derivatives from contaminated from liquid media.

4.1. Molecular modeling studies

The structural analysis for the Zearalenone ligand co-crystallized along with estrogen receptor alpha (ERα) (PDB code: 5krc) substrate-binding pocket revealed S-score of −14.8831 kcal/mol and hydrogen bond network comprising L387 and E353 [47] in-silico molecular modeling for the predicted iodindated zearalenone showed that all of them bind to the main pocket as zearalenone [co-crystallized ligand], as shown in (Fig. 6a, b).

The results of the docking study were as follow:

Monoiodo-zearalenone suggested structure (2a) has S-score of −13.5369 kcal/mol and had two hydrogen bonds with 2 different amino acids: one with E353 of distance (1.35 Aº), one with L346 of distance (1.34 Aº), as shown in (Fig. 7).

Diiodo- zearalenone suggested structure (2b) has S-score of −12.5866 kcal/mol and had one hydrogen bond with H524 of distance (2.44 Aº), as shown in (Fig. 7).

Monoiodo-zearalenone suggested structure (2c) has S-score of −12.2297 kcal/mol and had two hydrogen bonds with 2 different amino acids: one with E353 of distance (1.91 Aº), one with H524 of distance (2.45 Aº), as shown in (Fig. 7).

Conclusively, the presence of heavy iodine atom didn't disturb the binding ability of zearalenone to its target (5krc).

5. Conclusions

An optimized protocol for the synthesis of the radiotracer [125I]-iodo ZEA in high radiochemical yield of ≥ 98 % has been developed by electrophilic substitution mediated by Ch-T. About 98 % radio-labeling purity was observed to be stable in normal saline and rat serum. The biodistribution studies in two groups of normal and infected mice indicated that the radiotracer [125I]-iodo ZEA has the same distribution except in ovaries. It was also observed that [125I]-iodo ZEA accumulation declined in the ovaries at the group of mice taking L. plantarum, infected group from 3.22 % to 0.09 at 2 h p.i. Therefore, this current 298 work proposes a possible attempt to diminish the GIT absorption of ZEA and/or other mycotoxins from the human diet.

For ZEN which is a widespread mycotoxin contaminating cereal crops, a lot of worries concerning the hazards effects resulting from acute ingestion or chronic ingestion of insanitary food as a result of

Table 1
Biodistribution of ^{125}I-Zearalenone in normal mice at different times.

Organs & body fluids	% I.D./gram at different times post injection				
	5 min	15 min	30 min	60 min	120 min
Blood	13.0 ± 0.16	10.2 ± 0.18	5.27 ± 0.18	2.0 ± 0.2	1.1 ± 0.1
Bone	1.14 ± 0.11	1.2 ± 0.1	1.11 ± 0.1	0.95 ± 0.02	0.90 ± 0.01
Muscle	3.6 ± 0.1	2.90 ± 0.2	2.00 ± 0.1	1.60 ± 0.1	1.00 ± 0.2
Brain	0.78 ± 0.01	0.70 ± 0.02	0.60 ± 0.01	0.55 ± 0.01	0.46 ± 0.01
Lungs	1.20 ± 0.11	1.30 ± 0.1	1.1 ± 0.15	0.91 ± 0.02	0.80 ± 0.01
Heart	1.00 ± 0.11	1.2 ± 0.12	0.91 ± 0.01	0.88 ± 0.02	0.80 ± 0.01
Liver	14.16 ± 0.17	18.60 ± 0.67	25.29 ± 0.25	38.24 ± 0.79	27.15 ± 1.10
Kidneys	5.17 ± 0.19	7.27 ± 0.99	10.25 ± 0.48	6.19 ± 0.89	3.11 ± 0.55
Spleen	1.11 ± 0.11	1.21 ± 0.14	1.25 ± 0.13	1.00 ± 0.11	0.89 ± 0.03
Intestine	12.4 ± 0.55	15.9 ± 0.66	29.14 ± 0.18	38.0 ± 0.78	45.8 ± 1.40
Stomach	1.11 ± 0.13	1.15 ± 0.12	1.0 ± 0.11	0.95 ± 0.01	0.90 ± 0.02
Ovary	2.50 ± 0.02	3.6 ± 0.03	8.8 ± 0.02	7.33 ± 0.01	3.22 ± 0.01

Mean±SEM (mean of five experiments).

Table 2
Biodistribution of ^{125}I-Zearalenone in normal mice bearing acid lactic bacteria at different times.

Organs & body fluids	% I.D./gram at different times post injection				
	5 min	15 min	30 min	60 min	120 min
Blood	13.9 ± 0.17	11.1 ± 0.19	6.33 ± 0.17	3.0 ± 0.13	1.4 ± 0.11
Bone	1.15 ± 0.14	1.3 ± 0.09	1.00 ± 0.12	1.10 ± 0.13	0.98 ± 0.07
Muscle	3.1 ± 0.14	2.60 ± 0.16	2.21 ± 0.15	1.80 ± 0.12	1.10 ± 0.11
Brain	0.69 ± 0.02	0.72 ± 0.05	0.59 ± 0.06	0.50 ± 0.04	0.49 ± 0.01
Lungs	1.14 ± 0.11	1.20 ± 0.12	1.11 ± 0.13	0.95 ± 0.09	0.90 ± 0.08
Heart	1.12 ± 0.13	1.14 ± 0.12	1.00 ± 0.11	0.96 ± 0.1	0.91 ± 0.09
Liver	12.15 ± 0.19	17.77 ± 0.96	28.21 ± 1.87	36.20 ± 1.22	30.19 ± 0.22
Kidneys	4.16 ± 0.19	6.55 ± 0.33	9.21 ± 0.62	7.26 ± 0.27	2.98 ± 0.11
Spleen	1.17 ± 0.14	1.25 ± 0.15	1.20 ± 0.12	1.11 ± 0.11	1.00 ± 0.13
Intestine	11.5 ± 0.27	14.8 ± 0.59	30.15 ± 0.19	39.0 ± 0.55	46.1 ± 1.22
Stomach	1.00 ± 0.12	1.10 ± 0.13	0.95 ± 0.09	0.92 ± 0.08	0.90 ± 0.09
Ovary	0.11 ± 0.01	0.15 ± 0.02	0.22 ± 0.01	0.20 ± 0.03	0.09 ± 0.02

Mean±SEM (mean of five experiments).

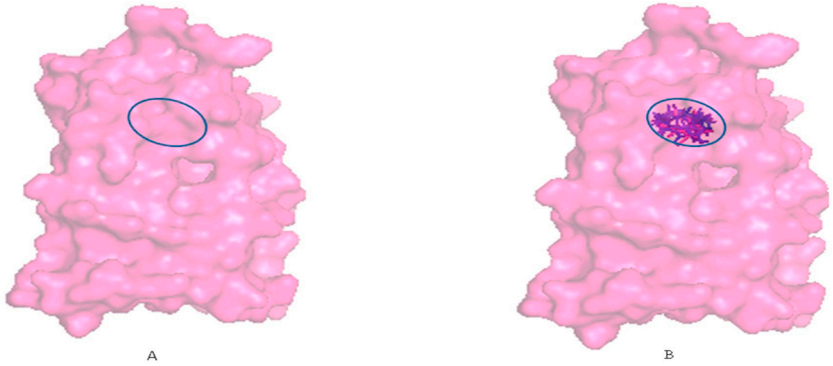

Fig. 6. A) The violet circle is the main binding pocket of zearalenone co-crystalized ligand on (ERα) (PDB code: 5krc), B) Overlay of all the iodinated proposed structures and zearalenone on (ERα).

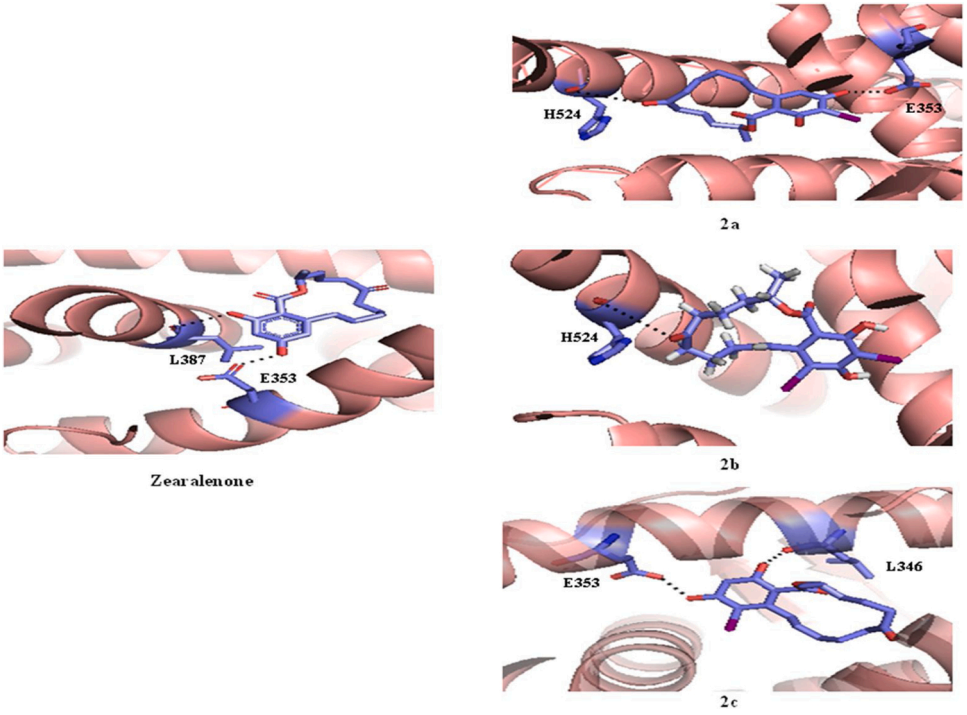

Fig. 7. 3D presentation of : **zearalenone** on (ERα) (PDB code: 5krc) showing the 2 H-bonds (dotted black line) with L387 and E353, show **2a** with 2H- bonds (dotted black line) with H524 and E353 show **2b** with one H- bond (dotted black line) with H524 and last **2c** with 2 H-bonds (dotted black line) with L346 and E353.

mycotoxin contamination. This current work proposes a possible attempt to diminish the GIT absorption of ZEN and/or other mycotoxins from the human diet.

Authorship statement

All persons who have made substantial contributions to the work but do not meet the criteria for authorship are listed in Acknowledgments section (technical help, writing assistance, general support, financial and material support).

Research funding

None declared.

Conflict of interest

The authors declare no conflict of interest.

Data availability

Data will be made available on request.

Declaration of Competing Interest

The authors report no declarations of interest.

References

[1] C. Gruber-Dorninger, T. Jenkins, G. Schatzmayr, Global mycotoxin occurrence in feed: a ten-year survey, Toxins (Basel) 11 (2019) 375.
[2] G.G. Kuiper, J.G. Lemmen, B. Carlsson, J.C. Corton, S.H. Safe, P.T. van Der Saag, B. van Der Burg, J.Å. Gustafsson, Interaction of estrogenic chemicals and phytoestrogens with estrogen receptor β, Endocrinology 139 (1998) 4252–4263.
[3] P. Chattopadhyay, A. Pandey, D. Goyary, A. Chaurasia, L. Singh, V. Veer, Technetium-99m-labeled deoxynivalenol from Fusarium mycotoxin alters organ toxicity in mice, J. Venom. Anim. Toxins Incl. Trop. Dis. 18 (2012) 258–263.
[4] A.A. Onilude, O.E. Fagade, M.M. Bello, I.F. Fadahunsi, Inhibition of aflatoxin-producing aspergilli by lactic acid bacteria isolates from indigenously fermented cereal gruels, Afr. J. Biotechnol. 4 (12) (2005) 1404–1408.

[5] A. Laitila, H.L. Alakomi, L. Raaska, T. Mattila-Sandholm, A. Haikara, Antifungal activities of two Lactobacillus plantarum strains against Fusarium moulds in vitro and in malting of barley, J. Appl. Microbiol. 93 (2002) 566–576.

[6] A. Savadogo, C.A.T. Ouattara, I.H.N. Bassole, S.A. Traore, Bacteriocins and lactic acid bacteria – a mini review, Afr. J. Biotechnol. 5 (2006) 678–683.

[7] F. Bovo, C. Corassin, R. Rosim, C.F. de Oliveira, Efficiency of lactic acid bacteria strains for decontamination of aflatoxin M1 in phosphate buffer saline solution and in skimmed milk, Food Bioprocess Technol. 6 (2013) 2230–2234.

[8] M.L. Suarez-Quiroz, O. Gonzalez-Rios, E.I. Champion-Martinez, O. Angulo, Effects of lactic acid bacteria isolated from fermented coffee (Coffea arabica) on growth of Aspergillus ochraceus and ochratoxin A production, in: Proceedings of 22nd International Conference on Coffee Science, ASIC 14-19 September 2008; Campinas, SP Brazil, Paris: Association Scientifique Internationale du Café (ASIC), 2008, pp. 542–546.

[9] V. Niderkorn, H. Boudra, D.P. Morgavi, Binding of Fusarium mycotoxins by fermentative bacteria in vitro, J. Appl. Microbiol. 2006 (101) (2006) 849–856.

[10] S. Abbès, J.B. Salah-Abbès, H. Sharafi, R. Oueslati, K.A. Noghabi, Lactobacillus paracasei BEJ01 prevents immunotoxic effects during chronic zearalenone exposure in Balb/c mice, Immunopharmacol. Immunotoxicol. 35 (2013) 341–348.

[11] Z.Y. Zou, Z.F. He, H.J. Li, P.F. Han, X. Meng, Y. Zhang, F. Zhou, K.P. Ouyang, X. Y. Chen, J. Tang, In vitro removal of deoxynivalenol and T-2 toxin by lactic acid bacteria, Food Sci. Biotechnol. 21 (2012) 1677–1683.

[12] S. Hawar, W. Vevers, S. Karieb, B.K. Ali, R. Billington, J. Beal, Biotransformation of patulin to hydroascladiol by Lactobacillus plantarum, Food Control 34 (2013) 502–508.

[13] A. Zinedine, M. Faid, M. Benlemlih, In vitro reduction of aflatoxin B1 by strains of lactic acid bacteri isolated from Moroccan sourdough bread, Int. J. Agric. Biol. 7 (2005) 67–70.

[14] M. Piotrowska, Z. Zakowska, The elimination of ochratoxin A by lactic acid bacteria strains, Pol. J. Microbiol. 54 (2005), 279-.

[15] H. El-Nezami, N. Polychronaki, Y.K. Lee, C. Haskard, R. Juvonen, S. Salminen, H. Mykkänen, Chemical moieties and interactions involved in the binding of zearalenone to the surface of Lactobacillus rhamnosus strains GG, J. Agric. Food Chem. 52 (2004) 4577–4581.

[16] S. Hatab, T. Yue, O. Mohamad, Removal of patulin from apple juice using inactivated lactic acid bacteria, J. Appl. Microbiol. 112 (2012) 892–899.

[17] M.H. Sanad, G.M. Saleh, F.A. Marzook, Radioiodination and biological evaluation of nizatidine as a new highly selective radiotracer for peptic ulcer disorder detection, J. Label Compd. Radiopharm. 60 (2017) 600–607.

[18] M.H. Sanad, A.S.M. Fouzy, M. Sobhy Hassan, S. Hathout Amal, A. Hussainb Omaima, Tracing the protective activity of Lactobacillus plantarum using technetium-99m labeled zearalenone for organ toxicity, Int. J. Radiat. Biol. 94 (12) (2018) 1151–1158.

[19] M.H. Sanad, S.B. Challan, Radioiodination and biological evaluation of rabeprazole as a peptic ulcer localization radiotracer, Radiochemistry 59 (3) (2017) 307–312.

[20] A.M. Amin, M.H. Sanad, S.M. Abd-Elhaliem, Radiochemical and biological characterization of 99m Tc-piracetam for brain imaging, Radiochemistry 55 (6) (2013) 624–628.

[21] O.A. El-Kawy, M.H. Sanad, F. Marzook, 99mTc-mesalamineas potential agent for diagnosis and monitoring of ulcerative colitis: labelling, characterisation and biological evaluation, J. Radioanal. Nucl. Chem. 308 (1) (2016) 279–286.

[22] M.H. Sanad, A.M. Amin, Optimization of labeling conditions and bioevalution of 99mTc-meloxicam for inflammation imaging, Radiochemistry 55 (5) (2013) 521–526.

[23] M.H. Sanad, T.M. Sakr, H.A.A. Walaa, E.A. Marzook, In silico study and biological evaluation of 99mTc-tricabonyl oxiracetam as a selective imaging probe for AMPA receptors, J. Radioanal. Nucl. Chem. 314 (3) (2017) 1505–1515.

[24] Molecular Operating Environment (MOE). 2016. Chemical Computing Group Inc., 1010 Sherbooke St. West, Suite #910, Montreal, QC, Canada., H3A, 2R7.2019.

[25] L. Paul, Protonate3D: assignment of ionization states and hydrogen coordinates to macromolecular structures, Proteins 75 (2009) 187–205.

[26] M. Naïm, S. Bhat, K.N. Rankin, S. Dennis, S.F. Chowdhury, I. Siddiqi, P. Drabik, T. Sulea, C.I. Bayly, A. Jakalian, E.O. Purisima, Solvated interaction energy (SIE) for scoring protein-ligand binding affinities. 1. Exploring the parameter space, J. Chem. Inf. Model. 47 (2007) 122–133.

[27] V.J. Jennings, E. Bishop, Analytical applications of chloramine-T, Crit. Rev. Anal. Chem. 3 (4) (1973) 407–419.

[28] B.C. Basavaraju, M.N. Kumara, M. Harsha, B.M. Chandrashekara, Mechanistic investigation of oxidative decolorization of an azo dye metanil yellow by chloramine - T in hydrochloric acid medium: a spectrophotometric approach, Int. J. Res. Appl. Sci. Eng. Technol. 6 (1) (2018) 2165–2172.

[29] V. Aiko, P. Edamana, A. Mehta, Decomposition and detoxification of aflatoxin B1 by lactic acid, J. Sci. Food Agric. 96 (2016) 1959–1966, https://doi.org/10.1002/jsfa.7304.

[30] J.W. Bennett, M. Klich, Mycotoxins, Clin. Microbiol. Rev. 16 (2003) 497–516.

[31] T. Kuiper-Goodman, P.M. Scott, H. Watanabe, Risk assessment of the mycotoxin zearalenone, Regul. Toxicol. Pharmacol. 7 (1987) 253–306.

[32] Z.P. Zhuang, M.P. Kung, C. Hou, K. Ploessl, H.F. Kung, Biphenyls labeled with technetium 99m for imaging beta-amyloid plaques in the brain, Nucl. Med. Biol. 32 (2005) 171–184.

[33] X. Chen, Y. Guo, Q. Zhang, G. Hao, H. Jia, B. Liu, Preparation and biological evaluation of 99mTc-CO-MIBI as myocardial perfusion imaging agent, Organomet Chem. 693 (2008) 1822–1828.

[34] M.H. Sanad, I.T. Ibrahim, Radiodiagnosis of peptic ulcer with technetium -99m labeled rabeprazole, Radiochemistry 57 (2015) 425–430.

[35] M.H. Sanad, H.M. Talaat, Radiodiagnosis of peptic ulcer with technetium-99m-labeled esomeprazole, Radiochemistry 59 (2017) 396–401.

[36] M.H. Sanad, K.M. Sallam, F. Marzook, Labeling and biological evaluation of 99mTc-tricarbonyl-chenodiol for hepatobiliary Imaging1, Radiochemistry 59 (2017) 525–529.

[37] M.H. Sanad, D.H. Salama, F.A. Marzook, Radioiodinated famotidine as a new highly selective radiotracer for peptic ulcer disorder detection, diagnostic nuclear imaging and biodistribution, Radiochim. Acta 105 (5) (2017) 389–398.

[38] E.H. Borai, M.H. Sanad, A.S.M. Fouzy, Optimized chromatographic separation and biological evaluation of 99mTc-clarithromycin for infective inflammation diagnosis, Radiochemistry 58 (1) (2016) 84–91.

[39] J.J. Pestka, Z. Islam, C.J. Amuzie, Immunochemical assessment of deoxynivalenol tissue distribution following oral exposure in the mouse, Toxicol. Lett. 178 (2008) 83–87.

[40] B.S. Shin, S.H. Hong, J.B. Bulitta, J.B. Lee, S.W. Hwang, H.J. Kim, S.D. Yang, H.-S. Yoon, D.J. Kim, B.M. Lee, et al., Physiologically based pharmacokinetics of zearalenone, J. Toxicol. Environ. Health Part A 72 (2009) 1395–1405.

[41] IACR, Some traditional herbal medicines, some mycotoxins, naphthahene and styrene. Monographs on the Evaluation of Carcinogenic Risks to Humans, IARS Press, Lyon, 2002, p. 556.

[42] J. Yang, Y. Zhang, Y. Wang, S. Cui, Toxic effects of zearalenone and alpha-zearalenol on the regulation of steroidogenesis and testosterone production in mouse Leydig cells, Toxicol. In Vitro 21 (2007) 558–565.

[43] N. Wang, W. Wu, J. Pan, M. Long, Detoxification strategies for zearalenone using microorganisms: a review, Microorganisms 7 (2019) 208.

[44] P. Horky, S. Skalickova, D. Baholet, J. Skladanka, Nanoparticles as a solution foreliminating the risk of mycotoxins, Nanomaterial 8 (2018) 1–21.

[45] V. Niderkorn, D.P. Morgavi, E. Pujos, A. Tissandier, H. Boudra, Screening of fermentative bacteria for their ability to bind and biotransform deoxynivalenol, ZEA and fumonisins in an in vitro simulated corn silage model, Food Addit. Contamin. 24 (2007) 406–415.

[46] H. El-Nezami, N. Polychronaki, S. Salminen, H. Mykk€anen, Binding rather than metabolism may explain the interaction of two food grade Lactobacillus strains with ZEA and its derivative a-zearaclenol, Appl. Environ. Microbiol. 68 (2002) 3545–3549.

[47] Jerome C. Nwachukwu, Sathish Srinivasan, Nelson E. Bruno, Olivier Elemento, John A. Katzenellenbogen, Kendall W. Nettles, Systems structural biology analysis of ligand effects on ER alpha predicts cellular response to environmental estrogens and anti-hormone therapies, Cell Chem. Biol. 24 (2017) 35–45.

[48] M.H. Sanad, K.M. Sallam, F.A. Marzook, S.M. Abd-Elhaliem, Radioiodination and biological evaluation of candesartan as a tracer for cardiovascular disorder detection, J. Label. Compd. Radiopharm. 59 (2016) 484.

[49] M.H. Sanad, A.M. Ebtisam, B.C. Safaa, Radioiodination of olmesartan medoxomil and biological evaluation of the product as a tracer for cardiac imaging, Radiochim. Acta 106 (2018) 329.

[50] I.T. Ibrahim, M.H. Sanad, Radiolabeling and biological evaluation of losartan as a possible cardiac imaging agent, Radiochemistry 55 (2013) 336.

[51] B.C. Safaa, A.M. Fawzy, M. Ayman, Synthesis of radioiodinated carnosine for hepatotoxicity imaging induced by carbon tetrachloride and its biological assessment in rats, Radiochim. Acta 108 (2021) 397.

[52] A. Massoud, S.B. Challan, N. Maziad, Characterization of polyvinylpyrrolidone (PVP) with technetium-99m and its accumulation in mice, J. Macromol. Sci. A. 58 (2022) 408–418.

[53] M.H. Sanad, H.B. Emad, Comparative biological evaluation between ^{99m}Tc tricarbonyl and 99mTc-Sn(II) levosalbutamol as a β2-adrenoceptor agonist, Radiochim. Acta 103 (2015) 879.

[54] A. Massoud, S.A. Waly, F. Abou El-Nour, Removal of U (VI) from simulated liquid waste using synthetic organic resin, Radiochemistry 59 (2017) 272–279.

[55] M.H. Sanad, Labeling and biological evaluation of ^{99m}Tc-azithromycin for infective inflammation diagnosis, Radiochemistry 55 (2013) 539–544.

[56] M.H. Sanad, Labeling of omeprazole with technetium-99m for diagnosis of stomach, Radiochemistry 55 (2013) 605–609.

[57] M.H. Sanad, Novel radiochemical and biological characterization of ^{99m}Tc-histamine as a model for brain imaging, J. Anal. Sci. Technol. 5 (2014) 23.

[58] M.H. Sanad, M. El-Tawoosy, Labeling of ursodeoxycholic acid with Technetium-99m for hepatobiliary imaging, J. Radioanal. Nucl. Chem. 298 (2013) 1105–1109.

[59] M.H. Sanad, I.T. Ibrahim, Radiodiagnosis of peptic ulcer with technetium-99m pantoprazole, Radiochemistry 55 (2013) 341–345.

[60] M.A. Motaleb, A.S.A. Adli, M. El-Tawoosy, M.H. Sanad, M. AbdAllah, An easy and effective method for synthesis and radiolabelling of risedronate as a model for bone imaging, J. Label Compd. Radiopharm. 59 (2016) 157–163.

[61] M.H. Sanad, D.H. Salama, F.A. Marzook, Radioiodinated famotidine as a new highly selective radiotracer for peptic ulcer disorder detection, diagnostic nuclear imaging and biodistribution, Radiochim. Acta 105 (2017) 389–398.

[62] I.Y. Abdel-Ghaney, M.H. Sanad, Synthesis of ^{99m}Tc-erythromycin complex as a model for infection sites imaging, Radiochemistry 55 (2013) 418–422.

[63] M.H. Sanad, A.I. Alhussein, Preparation and biological evaluation of ^{99m}Tc-N-histamine as a model for brain imaging: in silico study and preclinical evaluation, Radiochim. Acta 106 (2018) 229–238.

[64] M.H. Sanad, N. Farouk, A.S.M. Fouzy, Radiocomplexation and bioevaluation of ^{99m}Tc-nitrido-piracetam as a model for brain imaging, Radiochim. Acta 105 (2017) 729–737.

[65] M.H. Sanad, H.A. Shweeta, Preparation and bio-evaluation of 99mTc-carbonyl complex of ursodeoxycholic acid for hepatobiliary Imaging, J. Mol. Imag. Dyn. 5 (2015) 1–6.

[66] M.H. Sanad, H.B. Emad, Performance characteristics of biodistribution of 99mTc-cefprozil for in-vivo infection imaging, J. Anal. Sci. Technol. 5 (2014) 32.

[67] M.H. Sanad, M.A. Abelrahman, F.M.A. Marzook, Radioiodination and biological evaluation of levalbuterol as a new selective radiotracer: a β2-adrenoceptor agonist, Radiochim. Acta 104 (2016) 345–353.

[68] M.H. Sanad, A.B. Farag, H.S.J. Dina, Radioiodination and bioevaluation of rolipram as a tracer for brain imaging: in silico study, molecular modeling and gamma scintigraphy, J. Label Compd. Radiopharm. 61 (2018) 501–508.

[69] M.A. Motaleb, A.A. Selim, M. El-Tawoosy, M.H. Sanad, El-Hashash, MA, Synthesis, radiolabeling and biological distribution of a new dioxime derivative as a potential tumor imaging agent, J. Radioanal. Nucl. Chem. 314 (2017) 1517–1522.

[70] H.M. Sanad, A.A. Ibrahim, Radioiodination, diagnostic nuclear imaging and bioevaluation of olmesartan as a tracer for cardiac imaging, Radiochim. Acta 106 (2018) 843–850.

[71] M.E. Moustapha, M.A. Motaleb, M.H. Sanad, Synthesis and biological evaluation of ^{99m}Tc-labetalol for β1- adrenoceptor mediated cardiac imaging, J. Radioanal. Nucl. Chem. 309 (2016) 511–516.

[72] M.H. Sanad, A.A. Ibrahim, H.M. Talaat, Synthesis, bioevaluation and gamma scintigraphy of ^{99m}Tc-N-2-(Furylmethyl iminodiacetic acid) complex as a new renal radiopharmaceutical, J. Radioanal. Nucl. Chem. 315 (2018) 57–63.

[73] M.A. Motaleb, M.H. Sanad, A.A. Selim, M. El-Tawoosy, M.A. El-Hashash, Synthesis, characterization, radiolabeling and biodistribution of a novel cyclohexane dioxime derivative as a potential candidate for tumor imaging, Int. J. Radiat. Biol. 94 (2018) 590–596.

[74] M.H. Sanad, F.A. Marzook, S.M. Abd-Elhaliem, Radioiodination and biological evaluation of irbesartan as a tracer for cardiac imaging, Radiochim. Acta 109 (2021) 41–46.

[75] M.H. Sanad, A.B. Farag, G.M. Saleh, Radiosynthesis and biological evaluation of 188Re-5,10,15,20–Tetra (4-pyridyl)-21H,23H-porphyrin complex as a tumor-targeting agent, Radiochemistry 61 (2019) 347–351.

[76] M.H. Sanad, H.M. Talaat, A.S.M. Fouzy, Radioiodination and biological evaluation of mesalamine as a tracer for ulcerative colitis imaging, Radiochim. Acta 106 (2018) 393–400.

[77] M.H. Sanad, K.M. Sallam, D.H. Salama, ^{99m}Tc-Oxiracetam as a potential agent for diagnostic imaging of brain: labeling, characterization, and biological evaluation, Radiochemistry 60 (2018) 58–63.

[78] M.A. Motaleb, M.H. Sanad, Preparation and quality control of 99mTc-6-{[2-amino- 2-(4 hydroxyphenyl)-acetyl]amino}-3,3- dimethyl- 7-oxo- 4-thia- 1-aza-bicyclo-heptane- 2-carboxylic acid complex as a model for detecting sites of infection, Arab J. Nucl. Sci. Appl. 45 (2012) 71–77.

[79] M.H. Sanad, F.A. Rizvi, R.R. Kumar, Radiosynthesis and bioevaluation of ranitidine as highly selective radiotracer for peptic ulcer disorder detection, Radiochemistry 62 (2020) 119–124.

[80] M.H. Sanad, E.A. Marzook, O.A. El-Kawy, Radiochemical and biological characterization of ^{99m}Tc-Oxiracetam as a model for brain imaging, Radiochemistry 59 (2017) 624–629.

[81] M.H. Sanad, B.C. Safaa, A.M. Fawzy, M.A.A. Sayed, A.M. Ebtisam, Radioiodination and biological evaluation of cimetidine as a new highly selective radiotracer for peptic ulcer disorder detection, Radiochim. Acta 109 (2021) 109–117.

[82] M.H. Sanad, F.A. Marzook, S. Gehan, A.B. Farag, H.M. Talaat, Radiolabeling, preparation, and bioevaluation of ^{99m}Tc-Azathioprine as a potential targeting agent for solid tumor imaging, Radiochemistry 61 (2019) 478–482.

[83] I.T. Ibrahim, S.M. Abdelhalim, M.H. Sanad, M.A. Motaleb, Radioiodination of 3-Amino-2-quinoxalinecarbonitrile 1,4- Dioxide and its biological distribution in erhlich ascites cancer bearing mice as a preclinical tumor imaging agent, Radiochemistry 59 (2017) 301–306.

[84] S.F.A. Rizvi, H. Zhang, S. Mehmood, M.H. Sanad, Synthesis of ^{99m}Tc-labeled 2Mercaptobenzimidazole as a novel radiotracer to diagnose tumor hypoxia, Transl. Oncol. 13 (2020) 100854.

[85] M.H. Sanad, T. Hanan, I.T. Ibrahim, S. Gehan, L.A. Abozaid, Radioiodinated celiprolol as a new highly selective radiotracer for β1-adrenoceptormyocardial perfusion imaging, Radiochim. Acta 106 (2018) 751–757.

[86] M.H. Sanad, H.M. Eyssa, N.M. Gomaa, F.A. Marzook, S.A. Bassem, Radioiodinated esomeprazole as a model for peptic ulcer localization, Radiochimica Acta. 109 (2021) 711–718.

[87] M.H. Sanad, F.A. Rizvi, R.R. Kumar, A.A. Ibrahim, Synthesis and preliminary biological evaluation of ^{99m}Tc-Tricarbonyl ropinirole as a potential brain imaging agent, Radiochemistry 61 (2019) 754–758.

[88] M.H. Sanad, S.F.A. Rizvi, A.B. Farag, Synthesis, characterization, and bioevaluation of ^{99m}Tc nitridooxiracetam as a brain imaging model, Radiochim. Acta 109 (2021) 477–483.

[89] M.A. Motaleb, M.H. Sanad, A.A. Selim, M. El-Tawoosy, M.A. El-Hashash, Synthesis, characterization, and radiolabeling of heterocyclic bisphosphonate derivative as a potential agent for bone imaging, Radiochemistry 60 (2018) 201–207.

[90] M.H. Sanad, M. El-Tawoosy, I.T. Ibrahim, Preparation and biological evaluation of ^{99m}Tc-Timonacic acid as a new complex for hepatobiliary imaging, Radiochemistry 59 (2017) 92–97.

[91] M.H. Sanad, M.M. Saad, A.S.M. Fouzy, F. Marzook, I.T. Ibrahim, Radiochemical and biological evaluation of ^{99m}Tc-Labeling of phthalic acid using ^{99m}Tc-Tricabonyl and ^{99m}Tc-Sn (II) as a model for potential hazards imaging, J. Mol. Imag. Dyn. 6 (2016) 1.

[92] M.H. Sanad, F. Ayman, H. Dina, Radioiodination, molecular modelling and biological evaluation of aniracetam as a tracer for brain imaging, Egypt. J. Rad. Sci. Applic. 30 (2017) 131–143.

[93] M.A. Motaleb, K.F. Wanis, M.H. Sanad, Synthesis, characterization and labeling of 2-{N, N-dicarboxymethyl (aminoacetyl)} aminothiazole with technetium-99m, Arab J. Nucl. Sci. Appli. 38 (2005) 137–145.

[94] M.A. Motaleb, K.F. Wanis, M.H. Sanad, Labeling and biological distribution of ^{99m}Tc-DCMA-AP, Arab J. Nucl. Sci. Appli. 39 (2006) 84–91.

[95] M.H. Sanad, M.A. Gizawy, M.A. Motaleb, I.T. Ibrahim, E.A. Saad, A comparative study between stannous chloride and sodium borohydrideas a reducing agents for the radiolabeling of 2,3,7,8,12,13,17,18-octaethyl-21H,23H-porphine with technetium-99m for tumor imaging, Radiochemistry 63 (2021) 507–514.

[96] M.H. Sanad, S.F.A. Rizvi, A.B. Farag, Radiosynthesis and in silico bioevaluation of 131I-Sulfasalazine as a highly selective radiotracer for imaging of ulcerative colitis, Chem. Biol. Drug Des. 98 (2021) 751–761.

[97] M.H. Sanad, A. Emam, S.H. Amal, H. Omaima, R. Magdy, F. Ahmed, Distribution of iodine125 labeled parathion and the protective effect of dried banana peel in experimental mice, Egyptian J. Chem. 65 (2022) 1–2.

[98] H.M. Sanad, A.B. Farag, M.A. Motaleb, Radioiodination and biological evaluation of landiolol as a tracer for myocardial perfusion imaging: preclinical evaluation and diagnostic nuclear imaging, Radiochim. Acta 106 (2018) 1001–1008.

[99] M.H. Sanad, S.F.A. Rizvi, A.B. Farag, Design of novel radiotracer ^{99m}TcN-tetrathiocarbamate as SPECT imaging agent: a preclinical study for GFR renal function, Chem. Pap. 76 (2) (2022) 1253–1263.

[100] M.H. Sanad, H.M. Eyssa, F.A. Marzook, et al., Radiosynthesis and biological evaluation of ^{99m}Tc-Nitrido-Levetiracetam as a brain imaging agent, Radiochemistry 63 (2021) 635–641.

[101] M.H. Sanad, H.M. Eyssa, F.A. Marzook, et al., Comparative bioevaluation of ^{99m}Tc-Tricarbonyl and 99mTc-Sn (II) Lansoprazole as a model for peptic ulcer localization, Radiochemistry 63 (2021) 642–650.

[102] M.H. Sanad, F.A. Marzook, S.F.A. Rizvi, A.B. Farag, A.S.M. Fouzy, Radioiodinated azilsartan as a new highly selective radiotracer for myocardial perfusion imaging, Radiochemistry 63 (2021) 520–525.

[103] M.H. Sanad, A.B. Farag, F.A. Marzook, S.K. Mandal, Preparation, characterization, and bioevaluation of ^{99m}Tc-famotidine as a selective radiotracer for peptic ulcer disorder detection in mice, Radiochim. Acta 110 (1) (2022) 67–74.

[104] M.H. Sanad, A.B. Farag, S.F.A. Rizvi, In silico and in vivo study of radio-iodinated nefiracetam as a radiotracer for brain imaging in mice, Radiochim. Acta 109 (2021) 575–582.

[105] A.S.A. El-Wetery, M.A.A. Fayz, M.H. Sanad, M.A.M. EI-Hashash, Study on the preparation of ^{99m}Tc-N-(pyrimidine-2-ylcarbamoyl methyl) iminodiacetic acid as a new complex for hepatobiliary imaging agent, Arab J. Nucl. Sci. Appli. 40 (2007) 109–118.

[106] M.H. Sanad, T.S. Hanan Gehan, In silico study and preclinical evaluation of radioiodinated procaterol as a potential scintigraphic agent for lung imaging, Egypt. J. Rad. Sci. Applic. 30 (2017) 117–130.

[107] M.H. Sanad, H.M. Eyssa, F.A. Marzook, S.F.A. Rizvi, A.B. Farag, A.S.M. Fouzy, A. B. Sabry, A.I. Alhussein, Synthesis, radiolabeling, and biological evaluation of 99mTc-Tricarbonyl mesalamine as a potential ulcerative colitis imaging agent, Radiochemistry 63 (6) (2021) 833–840.

[108] M.H. Sanad, H.M. Eyssa, F.A. Marzook, S.F.A. Rizvi, A.B. Farag, A.S.M. Fouzy, S. K. Mandal, S.S. Patnaik, Optimized chromatographic separation and bioevalution of radioiodinated ilaprazole as a new labeled compound for peptic ulcer localization in mice, Radiochemistry 63 (6) (2021) 811–818.

[109] M.H. Sanad, MSc thesis, Faculty of Science, Ain-Shams University, Cairo, Egypt, 2007.

[110] M.H. Sanad, MSc thesis, Faculty of Science, Zagazig University, Cairo, Egypt, 2004.

[111] M.H. Sanad, M.G. Nermien, M.E. Nermeen, T.I. Ismail, M. Ayman, Radioiodination of balsalazide, bioevaluation and characterization as a highly selective radiotracer for imaging of ulcerative colitis in mice, J. Label Compd. Radiopharm. (2022), https://doi.org/10.1002/JLCR.3961.

[112] M.H. Sanad, H.M. Eyssa, M.E. Heba, Enhancement of the thermal and physicochemical properties of styrene butadiene rubber composite foam using nanoparticle fillers and electron beam radiation, Radiochim. Acta (2022) 1091–2021, https://doi.org/10.1515/ract- 2021-1091.

[113] M.H. Sanad, Ulcerative colitis and peptic ulcer imaging, first ed., LAP LAMBERT Academic Publishing, Germany, 2017, pp. 1–160.

[114] M.H. Sanad, Nuclear medicine and brain imaging, first ed., LAP LAMBERT Academic Publishing, Germany, 2017, pp. 1–166.

[115] M.H. Sanad, E.A. Abdel Rahim, M.M. Rashed, A.S.M. Fouzy, A.H. Omaima, F. A. Marzook, S.M. Abd-Elhaliem, Radioiodination and biological evaluation of parathion as a new radiotracer to study in experimental mice, World J. Pharm. Pharm. Sci. 9 (2020) 148–158.

[116] F. Ayman, W. Ping, A. Mahmoud, S. Hesham, Biological and Medical Chemistry, 2021, p. 12003930, https://doi.org/10.26434/chemrxiv.

[117] H.E. Galal, M.F. Nahed, B. Ayman, A.A. Sheikha, Nucleosides, Nucleotides and Nucleic Acids 37 (2018) 186–198.

[118] A. Massoud, O.M. Farid, R.M. Maree, K.F. Allan, Z.R. Tian, An improved metal cation capture on polymer with graphene oxide synthesized by gamma radiation, React. Funct. Polym. 151 (2020) 104564.

[119] S.B. Challan, A. Massoud, Radiolabeling of graphene oxide by Tchnetium-99m for infection imaging in rats, J. Radioanal. Nucl. Chem. 314 (2017) 2189–2199.

[120] G.H. Elgemeie, N.M. Fathy, A.B. Farag, I.B. Yahab, Design and synthesis of new class indeno[1,2-b]pyridine thioglycosides, Nucleosides Nucleotides Nucleic Acids 39 (2020) 1–16.
[121] A.B. Farag, H.E. Ewida, M.S. Ahmed, Design, synthesis, and biological evaluation of novel amide and hydrazide based thioether analogs targeting Histone deacteylase (HDAC) enzymes, European J. Med. Chem. 148 (2018) 73–85.
[122] G.H. Elgemeie, N.M. Fathy, A.B. Farag, S.A. Kursani, Design, synthesis, molecular docking and anti-hepatocellular carcinoma evaluation of novel acyclic pyridine thioglycosides, Nucleosides Nucleotides Nucleic Acids 37 (2018) 186–198.
[123] A.B. Farag, A. Magdi, Spectrophotometric study of the interaction between a novel benzothiazolethioglycoside asantimicrobial agent with bovine serum albumin, Chem. Res. J. 2 (2017) 66–72.
[124] G.H. Elgemeie, A.B. Farag, Design, synthesis, and in vitro antihepatocellular carcinoma of novel thymine thioglycoside analogs as new antimetabolic agents, Nucleosides Nucleotides Nucleic Acids 36 (2017) 328–342.
[125] G.H. Elgemeie, N.M. Fathy, A.B. Farag, S.A. Kursani, Novel synthesis of dihydropyridine thioglycosides and their cyctotoxic activity, Nucleosides Nucleotides Nucleic Acids 36 (2017) 355–377.
[126] G.H. Elgemeie, N.M. Fathy, W.A. Zaghary, A.B. Farag, S-glycosides in medicinal chemistry: novel synthesis of cyanoethylene thioglycosides and their pyrazole derivatives, Nucleosides Nucleotides Nucleic Acids 36 (2017) 198–212.
[127] A.B. Farag, P. Wang, I. Boys, J. Schoggins, H. Sadek, Identification of Atovaquone, Ouabain and Mebendazole as FDA Approved drugs targeting SARS-COV -2, ChemRxiv (2020).
[128] R.L. White, C.M. White, H. Turgut, A. Massoud, Z.R. Tian, Comparative studies on copper adsorption by graphene oxide and functionalized graphene oxide nanoparticles, J. Taiwan Inst. Chem. Eng. 85 (2018) 18–28.
[129] S. Bekheet, M. El-Tawoosy, A. Massoud, I.H. Borei, H.M. Ghanem, 99mTc-labeled ceftazidime and biological evaluation in experimental animals for detection of bacterial infection, Am. J. Biochem. 4 (2014) 15–24.
[130] A. Massoud, H.E. Rizk, M.F. Attallah, Selective separation of Y(III) from Sr(II) using hybrid polymer: synthesis, characterization, batch and column study, Polym. Bull. 78 (2021) 7053–7069.
[131] M.M. Zaky, H.M. Eyssa, R.F. Sadek, Improvement of the magnesium battery electrolyte properties through gamma irradiation of nano polymer electrolytes doped with magnesium oxide nanoparticles, J. Vinyl Addit. Technol. 25 (2019) 243.
[132] M.M. Senna, H.A. Youssef, H.M. Eyssa, Effect of electron beam irradiation, EPDM and azodicarbonamide on the foam properties of LDPE sheet, Polym. Plast. Technol. Eng. 46 (2007) 1093.
[133] H.M. Eyssa, S.A. El Mogy, H.A. Youssef, Impact of foaming agent and nanoparticle fillers on the properties of irradiated rubber, Radiochim. Acta 109 (2021) 127.
[134] E.M. Hegazi, H.M. Eyssa, A.A. Abd El-Megeed, Effect of nanofiller on the ageing of rubber seal materials under gamma irradiation, J. Compos. Mater. 53 (2019) 2065.
[135] H.M. Eyssa, M. Osman, S.A. Kandil, M.M. Abdelrahman, Effect of ion and electron beam irradiation on surface morphology and optical properties of PVA, Nucl. Sci. Tech. 26 (2015) 060306.
[136] H.M. Eyssa, M.Y. Elnaggar, M.M. Zaky, Impact of graphene oxide nanoparticles and carbon black on the gamma radiation sensitization of acrylonitrile–butadiene rubber seal materials, Polym. Eng. Sci 61 (2021) 2843.
[137] H.A. Youssef, M.M. Senna, H.M. Eyssa, A. Sarhan, Fabrication of sponge nitrile butadiene rubber (NBR) by subsequent sulphur and electron beam irradiation, Mans. J. Chem. 37 (2010) 155.
[138] M.M. Senna, A.B. Mostafa, S.R. Mahdy, A.M. El-Naggar, Characterization of blend hydrogels based on plasticized starch/ cellulose acetate/carboxymethyl cellulose synthesized by electron beam irradiation, Nucl. Instrum. Methods Phys. Res. B 386 (2016) 22–29.
[139] H.M. Eyssa, S.G. Sawires, M.M. Senna, Gamma irradiation of polyethylene nanocomposites for food packaging applicationsagainst stored-product insect pests, J. Vinyl Addit. Technol. 25 (2019) 120.
[140] H.M. Eyssa, D.E. Abulyazied, M.A.M. Abo-State, Application of polyurethane /gamma-irradiated carbon nanotubes composites as antifouling coat, Polym. Compos. 39 (2018) E1196.
[141] H.M. Eyssa, W.S. Mohamed, M.M. El-Zayat, Irradiated rubber composite with nano and microfillers for mining rock application, Radiochim. Acta 107 (2019) 737.
[142] A.H. Youssef, M.M. Senna, H.M. Eyssa, Characterization of LDPE and LDPE/EVA blends crosslinked by electron beam irradiation and foamed with chemical foaming agent, J. Polym. Res. 14 (2007) 351.
[143] H.M. Eyssa, D.E. Abulyazied, M. Abdulrahman, H.A. Youssef, Mechanical and physical properties of nanosilica/nitrile butadienerubber composites cured by gamma irradiation, Egypt. J. Petro. 27 (2018) 383.
[144] H.A. Youssef, Y.K. Abdel-Monem, I.M. El-Sherbiny, H.M. Eyssa, H.M. El-Raheem, Effect of ionizing radiation on the properties of some synthesized polyurethanes, J. Pharm. Biol. Chem. Sci. 7 (2016) 855.
[145] H.M. Eyssa, M.S. Hassan, Surface characteristics of cotton/ polyester fabric coated with poly-urethane elastomers cured thermally or by using gamma irradiation, Egypt. J. Rad. Sci. Applic. 27 (2014) 91.